Check for
updates

Arctic Coralline Algae Elevate Surface pH and Carbonate in the Dark

Laurie C. Hofmann[1]*, Kathryn Schoenrock[2†] and Dirk de Beer[1]

[1] Max Planck Institute for Marine Microbiology, Microsensor Group, Bremen, Germany, [2] Department of Geographical and Earth Science, University of Glasgow, Glasgow, United Kingdom

Red coralline algae are projected to be sensitive to ocean acidification, particularly in polar oceans. As important ecosystem engineers, their potential sensitivity has broad implications, and understanding their carbon acquisition mechanisms is necessary for making reliable predictions. Therefore, we investigated the localized carbonate chemistry at the surface of Arctic coralline algae using microsensors. We report for the first time carbonate ion concentration and pH measurements ($[CO_3^{2-}]$) at and above the algal surface in the microenvironment. We show that surface pH and $[CO_3^{2-}]$ are higher than the bulk seawater in the light, and even after hours of darkness. We further show that three species of Arctic coralline algae have efficient carbon concentrating mechanisms including direct bicarbonate uptake and indirect bicarbonate use via a carbonic anhydrase enzyme. Our results suggest that Arctic corallines have strong biological control over their surface chemistry, where active calcification occurs, and that net dissolution in the dark does not occur. We suggest that the elevated pH and $[CO_3^{2-}]$ in the dark could be explained by a high rate of light independent carbon fixation that reduces respiratory CO_2 release. This mechanism could provide a potential adaptation to ocean acidification in Arctic coralline algae, which has important implications for future Arctic marine ecosystems.

Keywords: calcification, carbon concentrating mechanism, carbonate chemistry, light-independent carbon fixation, microenvironment, microsensor, rhodolith

INTRODUCTION

Red coralline algae play key roles as ecosystem engineers in global oceans (Foster, 2001; Nelson, 2009), and contribute significantly to carbonate deposition (Amado-Filho et al., 2012; Van Der Heijden and Kamenos, 2015). Some coralline algae, particularly crustose coralline algae, have shown sensitivity to ocean acidification in many laboratory and field studies (Hofmann and Bischof, 2014; McCoy and Kamenos, 2015), but it remains to be determined if they will have the capacity to adapt to the pH decrease and associated decrease in carbonate ion saturation states expected in future surface oceans due to higher dissolved CO_2 concentrations. In the polar oceans, especially the Arctic, where the carbonate buffering capacity is weak and the system is vulnerable to environmental change (Steinacher et al., 2009; Shadwick et al., 2013), coralline algae may be less resistant to ocean acidification than in lower latitudes, particularly during the dark Arctic winters (Büdenbender et al., 2011). However, recent studies have shown that some coralline algae alter their skeletal structure and composition (Nash et al., 2013; Ragazzola et al., 2013, 2016;

McCoy and Ragazzola, 2014; Kamenos et al., 2016) under elevated CO_2, perhaps in an effort to reduce skeletal dissolution, and they can have strong biotic control over calcification and inorganic carbon uptake (Comeau et al., 2013; Hofmann et al., 2016; Cornwall et al., 2017). It is becoming clear that Arctic coralline algae, particularly rhodoliths (free-living coralline red algal nodules), are more abundant than previously believed. For example, the existence of rhodoliths in eastern Greenland was first reported last year, where several rhodolith beds along the eastern Greenlandic coast were found (Jørgensbye and Halfar, 2017). The authors of this study suggest that there are likely many more beds in remote areas that are not close to research stations or settlements. Because rhodolith bed discoveries have been made around the world recently, the current estimates of the contribution of coralline algae to the global carbonate budget are likely severely underestimated, including their contribution to carbon storage (Van Der Heijden and Kamenos, 2015). Therefore, understanding the mechanism of calcification in polar coralline algae is necessary for making reliable predictions and subsequent policy decisions.
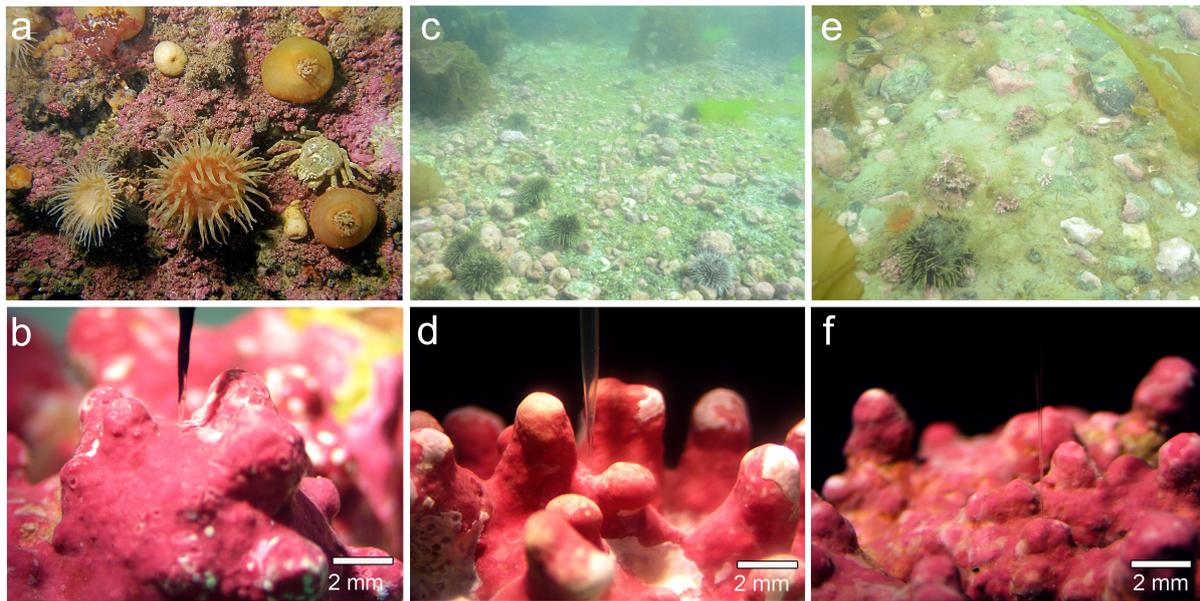
Coralline algae deposit high-Mg calcite in their cell walls, which cement filaments of cells together. They occur as either a thin crust on hard substrata (crustose coralline algae, CCA), as free-living rhodoliths, or as a flat thallus with articulated branches. The surface chemistry of dissolved inorganic carbon (DIC) in calcifying algae can be controlled by several processes. Photosynthesis, dominant in the light, leads to an increase of the pH and carbonate ion concentration $[CO_3^{2-}]$ and thus favors calcification, while net respiration has the opposite effect on calcification (McConnaughey, 1989). Calcification induces the liberation of protons (as $Ca^{2+} + HCO_3^- \rightarrow CaCO_3 + H^+$), and thus buffers the pH shift induced by photosynthesis, while dissolution can buffer the pH decrease by respiration (Gattuso et al., 1999). Active transport, mostly proton pumping or active uptake of HCO_3^- can induce pH shifts that are independent, and often of different time scales, as the metabolic processes (Borowitzka and Larkum, 1976; McConnaughey, 1991; de Beer and Larkum, 2001; Al-Horani et al., 2003). The latter can be considered as expression of biotic control of calcification (Borowitzka and Larkum, 1977). These ion pumps transport HCO_3^- and H^+ into the tissue in the light (Borowitzka and Larkum, 1987), where the enzyme carbonic anhydrase speeds up the dehydration of HCO_3^- to CO_2. Due to photosynthesis and the transport of protons away from the surface, the pH at the coralline algal surface (pH_S) is elevated compared to the bulk seawater pH (pH_B) (Hurd et al., 2011; Cornwall et al., 2013, 2015; Hofmann et al., 2016), which favors the surface calcification, due to higher CO_3^{2-} concentration. In the dark, the reverse process occurs, and the protons released are buffered by the CO_3^{2-} to form HCO_3^- (Comeau et al., 2013). Further evidence of elevated surface pH at the site of calcification in coralline algae has been shown in recent studies using boron isotopes (Cornwall et al., 2017; Donald et al., 2017). However, the dynamics of CO_3^{2-} and pH in response to light have never been measured at the surface of a coralline alga. Hence, no data on active processes that control the surface chemistry, like light-induced proton pumps, are available. To elucidate the possible presence of such pumps,

we measured the chemistry dynamics at the surface in response to illumination, using microsensors to achieve high-spatial resolution. For describing the complete carbonate system at the surface of coralline algae data on at least two parameters of the carbonate system are needed, assuming equilibrium. Therefore, we measured surface $[CO_3^{2-}]$ and pH using microsensors at the surface of polar coralline algae in response to light dynamics. Although these are not the ideal parameters to use for calculating the remaining parameters of the seawater carbonate system, we do so as a first attempt to provide a glimpse of what the surface chemistry of Arctic coralline algae may look like, considering it is not yet possible to measure DIC or total alkalinity (TA) directly at the algal surface. We hypothesized that surface $[CO_3^{2-}]$ would depend on light, being elevated in the light and reduced in the dark.

MATERIALS AND METHODS

Algae Sampling and Maintenance

Samples of the crustose coralline *Phymatolithon tenue* (Rosenvinge) Düwel & Wegeberg (**Figures 1a,b**) were collected between 10 and 12 m depth at Hansneset, off the southwestern coast of the island Bloomstrand in Kongsfjord, Svalbard, where temperatures range from −2 to 7°C during the year at 20 m depth (Laudien et al., 2014). High sediment deposition from surrounding glaciers results in high freshwater input and high turbidity in Kongsfjord during summer (Hajime and Kudoh, 1997; Hanelt et al., 2001), which strongly attenuates the solar radiation at depth in the fjord (Hanelt et al., 2001). The photosynthetically active radiation (PAR) available at 10 m depth is less than 10% of surface radiation (Cui et al., 2013). Algal samples were transported to the Max Planck Institute for Marine Microbiology (MPIMM), where they were maintained at 4°C in custom-made re-circulating aquaria (20 L) with natural seawater (34 psu) on an 18:6 h day/night cycle at 10 µmol photons $m^{-2} s^{-1}$ for 1 year prior to the experiments. One-third of the seawater in the recirculating tanks was replaced every 2 weeks. Two species of *Lithothamnion* rhodoliths, *L. glaciale* Kjellman (**Figures 1c,d**) and *L. tophiforme* (Esper) Unger (**Figures 1e,f**), were collected using SCUBA from two sites off the southwestern coast of Greenland: Købbe Fjord (*L. glaciale*: 64.14, −51.59) and Akia Penninsula (*L. tophiforme*: 64.193210, −51.908612). Surface currents in the Nuuk region exceed 1 m s^{-1} shortly before and after slack tide, therefore water flow in coralline habitats is due to tidal flux year round. The site at Akia Peninsula experiences flushing from Godthåbsfjord to the marine environment through small channels, while Købbefjord has an influx and outflux of primarily marine water. Currents at the benthos have not been measured due to logistical constraints, but the site at Akia Peninsula specifically has a great deal of sedimentation (**Figure 1e**), indicating flow significantly decreases with depth. The site at Akia Penninsula has high canopy cover of *Saccharina longicruris* (**Figure 1e**), while there is almost no defined canopy cover in Købbefjord, only spotty cover of *Agarum clathratum* (**Figure 1c**). Average mid-day summer light intensities at 10 m depth range measured with an Odyssey PAR logger (Dataflow

FIGURE 1 | Images from collection sites and examples of specimens investigated: **(a,b)** Kongsfjord, *P. tenue*; **(c,d)** Købbefjord, *L. glaciale*; and **(e,f)** Akia Penninsula, *L. tophiforme*. In **(c)**, high cover of the crustose coralline *Clathromorphum* sp. is apparent. The microsensors used. In **(c,d)**, the microsensor is positioned between nodes/branches. In **(f)**, the microsensor is positioned at the tip of a node. *In situ* photographs are from M. Schwanitz and K. Schoenrock. Microscopic photos taken by L. Hofmann.

Systems Ltd, Christchurch, NZ) ranged between 101 and 196 μmol photons m^{-2} s^{-1} at midday. After collection, these specimens were transported to the MPIMM via the University of Glasgow in ambient seawater at 4°C, and then maintained in custom-made recirculating aquaria in the same conditions as Svalbard collections for 9 months prior to the experiments.

Microsensor Construction

O$_2$ microsensors were made and used as described by Revsbech (1989), liquid ion exchange (LIX) pH and CO$_3^{2-}$ microelectrodes were constructed according to de Beer et al. (2008). The O$_2$ optode was calibrated with 0 and 100% air saturated seawater obtained by bubbling with nitrogen gas and compressed air, respectively. All calibrations were conducted at 4°C. The CO$_3^{2-}$ microelectrode was calibrated following the continuous titration method from Han et al. (2014) using natural seawater. To reduce air exposure, the calibration was conducted in a glass Schott bottle with a Teflon-sealed lid with custom made holes for the pH electrode, microelectrode, and reference electrode. The HCl titration solution was added by inserting a needle syringe through the Teflon membrane. The pH microelectrode was calibrated using pH$_{NST}$ 7.0 and 9.0 buffers (Fluka Analytical, Buchs, Switzerland). The measured pH values were then corrected to the total pH scale by subtracting 0.1 pH units for the seawater chemistry calculations. We acknowledge that certified reference material is preferred for calibrating pH, but the extreme sensitivity of our LIX pH microelectrodes and their incompatibility with some calibration standards did not allow this. Because of the uncertainty associated with NBS buffers and the resulting calculations of the seawater system, we report the

profiles of CO$_3^{2-}$ as ratios rather than absolute concentrations. The oxygen and pH electrodes had average tip diameters between 10 and 20 μm, and therefore minimal influence on the diffusional boundary layer (DBL) of the coralline algae measured.

Microprofiling

The experimental set-up used for microprofiling was the same described in Hofmann et al. (2016). Seawater was pumped through a plexiglass flow cell (19 cm × 9 cm × 9.5 cm) attached to a temperature-controlled reservoir at approximately 2 cm s^{-1} (judged by particle movement) and passed through a perforated wall at the entrance and exit of the flow chamber to create laminar flow at the algal surface. All experiments were conducted at 7°C. pH and CO$_3^{2-}$ microelectrodes and an oxygen optode were used to measure depth microprofiles from the surface of the algae into the overlying seawater under both saturating light (100 μmol photons m^{-2} s^{-1}) and dark conditions. Microprofiles of the three species were measured under steady state conditions. Up to four individuals from each species were measured on multiple occasions at multiple branch tips (due to variations in DBL thickness depending on morphology, only branch tips were used; see Results below), but complete datasets for all three parameters (pH, O$_2$, and CO$_3^{2-}$) could only be obtained on three replicates of each species due to broken/faulty sensors. In the light, a steady state signal was achieved after several minutes, while a dark adaptation period of at least 30 min was necessary before obtaining a steady signal with no noticeable change. In order to determine when the dark steady state was reached, O$_2$, pH, and CO$_3^{2-}$ at the surface of the algae were monitored continuously overnight (see Light dynamics subsection below).

Microprofiles of O_2, pH, and CO_3^{2-} for each individual were obtained by first positioning the sensors at the surface of the algal specimen by hand using a micromanipulator (Pyroscience, Aachen, Germany) with the aid of a stereomicroscope. Using the software Profix (Pyroscience, Aachen, Germany), the microelectrodes were then programed to run four consecutive profiles from the surface of the alga (position 0) into the overlying water column (position 800 µm) at 50 µm intervals. Microprofiles were conducted first under saturating light and steady state conditions. Microprofiles in the dark were then obtained following a dark adaptation period of at least 30 min, after which there was no noticeable change in the sensor signal. Because light and dark profiles were measured at the same location on the same individual at different time points, light was treated as a repeated factor with two levels (light, dark) for statistical analysis in this case (see below). Oxygen fluxes were calculated from the concentration profiles according to Fick's Law [see Hofmann et al. (2016)] using the diffusion coefficient 1.34×10^{-9} m^2 s^{-1} for seawater at 7°C and 35‰ salinity. The delta pH was calculated by subtracting the surface pH from the bulk seawater pH ($\Delta pH = pH_S - pH_B$), and surface ratios of CO_3^{2-} were calculated by dividing the surface concentration by the bulk seawater concentration.

Microprofiles of pH at the branch tip and base of rhodoliths showed that branch bases have thicker DBL than branch tips, and consequently, the pH between branches is slightly higher than in the bulk seawater above branch tips (**Supplementary Table S1**). In order to reduce the variation in profile data driven by morphological characteristics, we measured all profiles on branch tips of individual rhodoliths. By standardizing the location of profile measurements, we observed that there was no difference in the boundary layer thickness between the crustose or branched forms investigated (**Supplementary Table S1**).

Inhibition Experiments

The extracellular carbonic anhydrase inhibitor, acetazolamide (AZ), was used to test for carbonic anhydrase activity and its effect on surface chemistry of one of the species investigated in this study (*L. glaciale*). By inhibiting carbonic anhydrase, we could determine if surface pH was directly coupled to photosynthesis. Prior the addition of the inhibitor, a gross photosynthesis versus irradiance curve was generated to determine limiting and saturating light levels. Gross photosynthesis measurements were conducted using the light–dark shift method (Revsbech and Jørgensen, 1983, 1986), and the preparation of AZ was conducted following the methods by Hofmann et al. (2016). The curve was fit using the nonlinear least squares (nls) command in R with the equation from Eilers and Peeters (1988) that considers potential photoinhibition

$$ GP = \frac{I}{aI^2 + bI + c} $$

where GP is gross photosynthesis, I is the irradiance, and a, b, and c are the parameters estimated by the model. After fitting the model to the data, the light saturation point could be estimated by calculating the light intensity at which photosynthesis was

saturating. pH profiles and gross photosynthesis were measured at three and five light conditions, respectively, prior to and after the addition of AZ (final concentration 280 µM). The addition of AZ was made to the seawater reservoir while the pH sensor remained on the surface of the alga. Measurements were made after a steady state was reached. Unfortunately, we could only successfully complete this experiment on a single individual, and therefore the figures can be found in the **Supplementary Material**.

Statistical Analysis

The parameters of the seawater carbonate system were calculated from the pH (total scale) and CO_3^{2-} concentrations measured at the algal surface and in the bulk seawater using the package seacarb in R. To test for an effect of site/species and light on O_2 flux, ΔpH and $[CO_3^{2-}]_S$:$[CO_3^{2-}]_B$, a nonparametric test for repeated measures data in factorial designs was conducted in RStudio (version 0.98.1087) using the nparLD package (nonparametric analysis of longitudinal data in factorial experiments). This test was appropriate because more than one group of subjects (groups = species) was observed repeatedly over time (Noguchi et al., 2012). Light and dark profiles were measured on the same individual at the same location at different time points. Results of the ANOVA-type statistic are reported. To determine if surface $[CO_3^{2-}]$ and $[O_2]$ differed from bulk $[CO_3^{2-}]$ and $[O_2]$, independent t-tests were conducted separately for each response variable for each species and light condition.
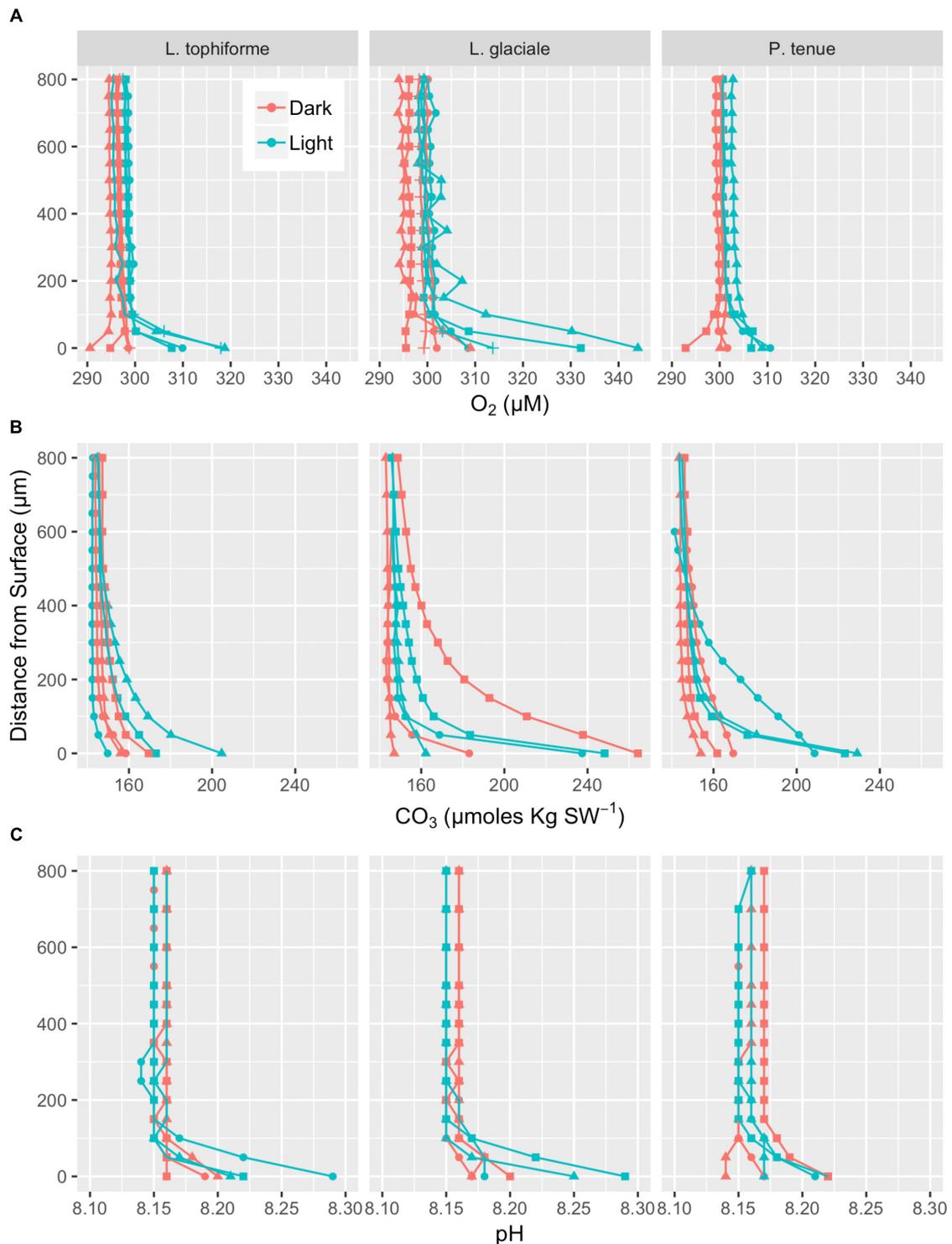
RESULTS

Oxygen, pH, and CO_3^{2-} Microprofiles

Microprofiles of O_2, CO_3^{2-}, and pH showed that despite reduced O_2 concentrations due to respiration in the dark, surface pH, and CO_3^{2-} concentrations both remained higher than the bulk seawater under both light and dark conditions (**Figures 2A–C**). This was observed on all three algal species. These trends are further shown by the ratio of $[CO_3^{2-}]_S$:$[CO_3^{2-}]_B$ and the delta pH (**Figures 3A,B**). There was no significant effect of site/species on either oxygen flux, ΔpH or $[CO_3^{2-}]_S$:$[CO_3^{2-}]_B$, but all parameters were significantly higher in the light than in the dark (O_2 flux: ANOVA-type statistic (ATS) = 62.5, $p = 2.7e - 15$ ΔpH: ATS = 18.5, $p = 1.7e-5$; $[CO_3^{2-}]_S$:$[CO_3^{2-}]_B$: ATS = 5.9, $p = 0.01$; see Statistical Analysis above).

The O_2 concentration at the surface was not significantly different from that of seawater in the dark, indicating that respiration rates (oxygen flux in the dark) were very low (**Figure 3C** and **Supplementary Table S2**). In the light, the surface concentration of O_2 significantly increased due to photosynthesis and a small efflux into the bulk seawater was observed (**Figure 3D** and **Supplementary Table S2**).

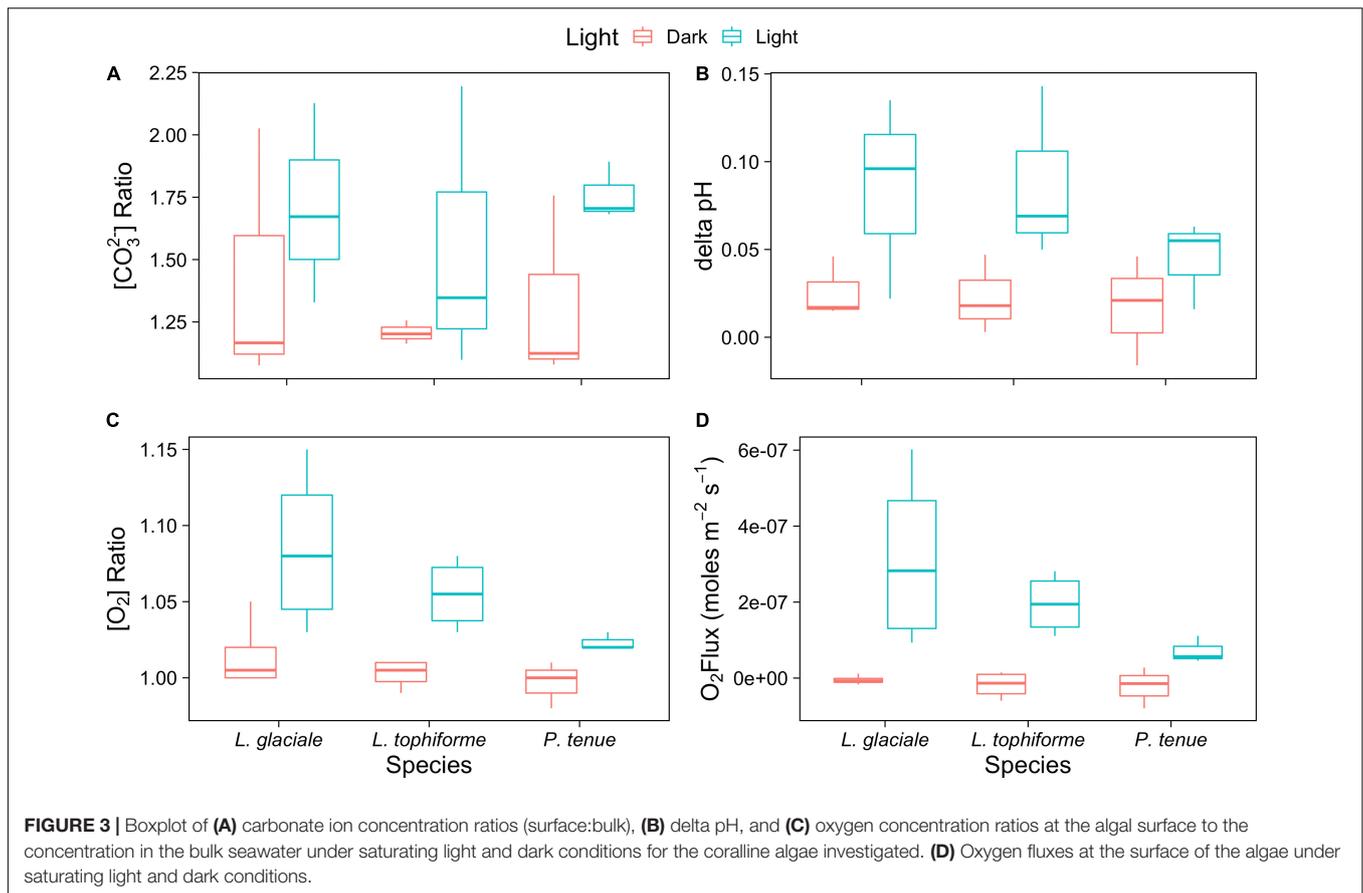## Surface Carbonate Chemistry

To assess the effect of light and darkness on the surface chemistry, we measured the dynamics of surface pH and $[CO_3^{2-}]$ in response to saturating light and darkness. Both surface pH

FIGURE 2 | Microprofiles of oxygen concentration **(A)**, carbonate ion concentration **(B)**, and pH **(C)** measured with microsensors under saturating light (blue) and dark (red) conditions. Each profile is an average of four replicate profiles ± SE. The symbols represent measurements conducted on different individual algae.

and $[CO_3^{2-}]$ increased in the light and decreased in the dark at the surface of *L. glaciale* from Købbe Fjord (**Figure 4**). Upon illumination, the $[CO_3^{2-}]_S$ increased sharply, and then

slowly decreased before reaching steady state at a level that always remained above the levels in darkness (**Figure 4**). However, after darkening, the pH slightly increased before

FIGURE 3 | Boxplot of **(A)** carbonate ion concentration ratios (surface:bulk), **(B)** delta pH, and **(C)** oxygen concentration ratios at the algal surface to the concentration in the bulk seawater under saturating light and dark conditions for the coralline algae investigated. **(D)** Oxygen fluxes at the surface of the algae under saturating light and dark conditions.
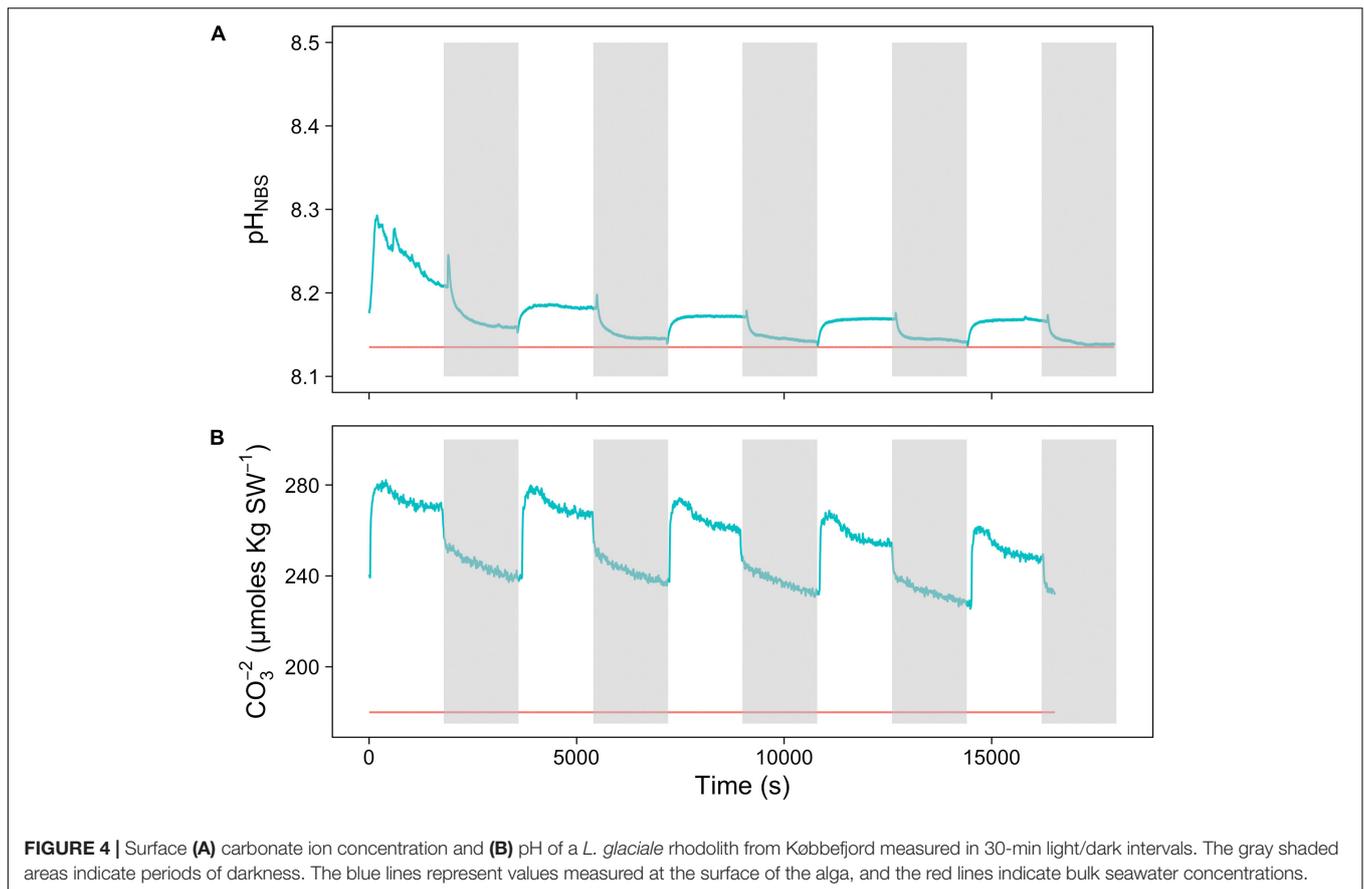
beginning to decrease and reaching a steady state. The opposite pattern was seen when the light was switched on, showing a slight dip in pH before it started increasing, and reaching a steady state. Regardless of whether the alga was in the light or dark, the pH_S, and $[CO_3^{2-}]_S$ always remained above the bulk seawater levels. Similar trends in light/dark dynamics were found for *P. tenue* and *L. tophiforme* (**Supplementary Figures S1, S2**). In order to determine when the $[O_2]_S$, pH_S, and $[CO_3^{2-}]_S$ reached steady state in the dark and to determine if they reach levels below the bulk seawater at any point, we monitored each parameter in the dark for up to 15 h. In *P. tenue* from Spitsbergen, the pH_S never dropped below pH_B in the dark, and the $[CO_3^{2-}]_S$ remained above $[CO_3^{2-}]_B$ for over 13 h, despite lower $[O_2]_S$ compared to $[O_2]_B$ (**Figure 5**). Similar patterns were found during extended periods of darkness for additional individuals of *P. tenue* and for *L. tophiforme* (**Supplementary Figures S3, S4**), although the pH_S dipped slightly below the pH_B in one specimen of *P. tenue* after 7 h (**Supplementary Figure S3**). From the pH and CO_3^{2-}, we calculated the remaining parameters of the carbonate system at the algal surface and in the bulk seawater using the package seacarb in R (see Materials and Methods). **Figure 6** shows that the surface DIC, pCO_2, HCO_3^-, and TA remained lower than the bulk seawater, while the aragonite saturation state remained higher than the bulk seawater.

Inhibition of Carbonic Anhydrase

The addition of AZ resulted in a slight decrease in surface O_2 and in surface pH of *L. glaciale* (**Supplementary Figure S5**). The inhibition of carbonic anhydrase only inhibited delta pH at 85 μmol photons m^{-2} s^{-1} (**Supplementary Figure S6**), which was below light saturation. The light at which gross photosynthesis was saturating before AZ addition was 130 μmol photons m^{-2} s^{-1} (**Supplementary Figure S7**). Carbonic anhydrase inhibition resulted in the inhibition of gross photosynthesis, which showed different patterns depending on light intensity. CA inhibition was constant above 10 μmol photons m^{-2} s^{-1} at approximately 50–75%. Only at the lowest light level (2 μmol photons m^{-2} s^{-1}), no inhibition was observed. This indicates that at only very low light intensities, the supply of CO_2 by transport from the seawater (13 μM) and non-catalyzed conversion of HCO_3^- is sufficient. However, at higher light intensities, and thus at higher photosynthetic capacity, CO_2 supply from the seawater limits the photosynthetic rate, and CA is needed to enhance the CO_2 supply (**Supplementary Figure S7**).

DISCUSSION

Our results show the carbonate chemistry conditions in the microenvironment of Arctic coralline algae. We did not observe

FIGURE 4 | Surface **(A)** carbonate ion concentration and **(B)** pH of a *L. glaciale* rhodolith from Købbefjord measured in 30-min light/dark intervals. The gray shaded areas indicate periods of darkness. The blue lines represent values measured at the surface of the alga, and the red lines indicate bulk seawater concentrations.
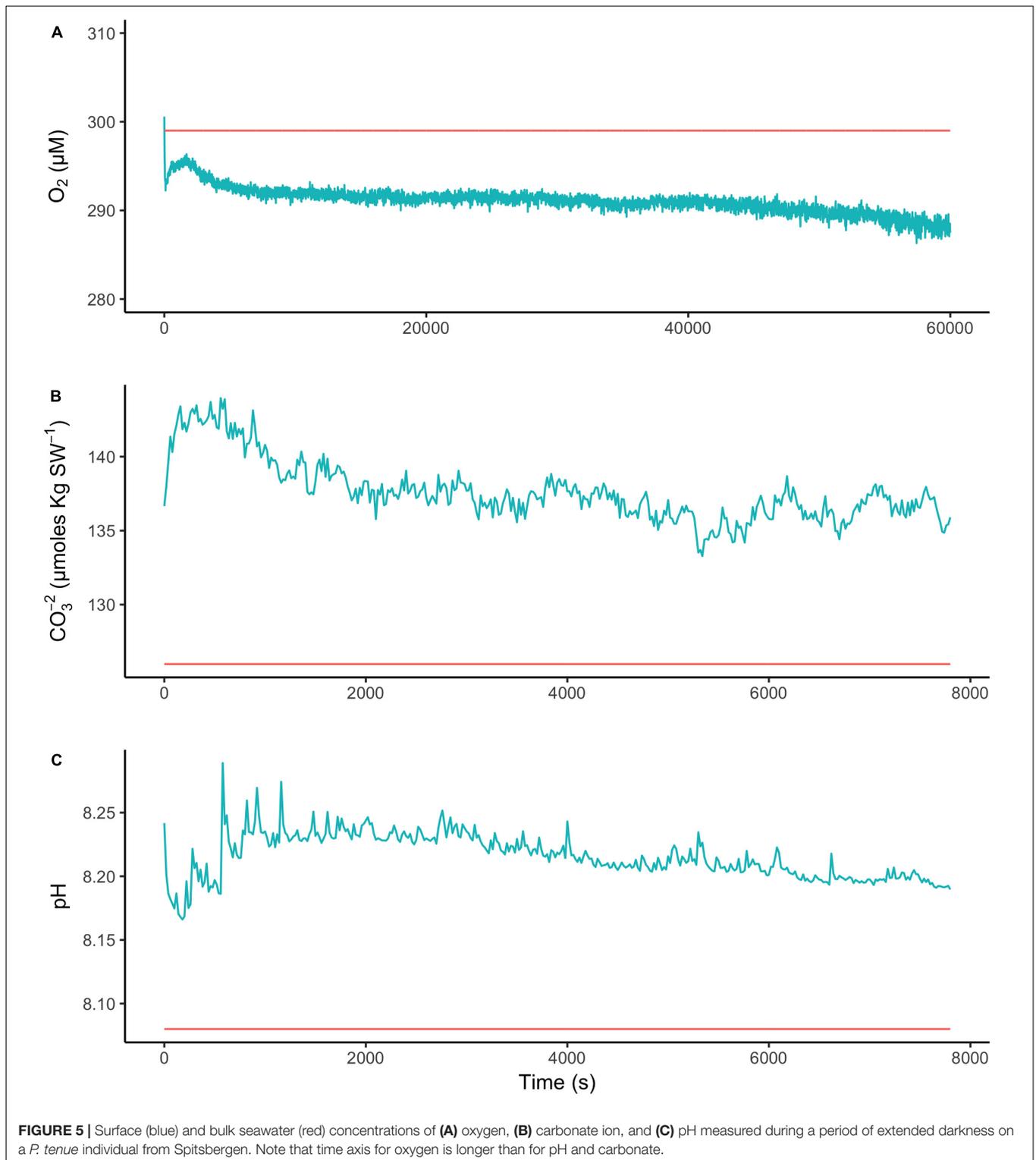
strong differences in pH_S or $[CO_3^{2-}]_S$ between the three species, indicating that in this case, the rhodolith versus crustose morphology did not have a strong influence on surface chemistry. Also, it suggest that our observations may hold generally for Arctic rhodoliths. The saturation state of calcite and aragonite remained greater than 1 under all conditions, despite respiration in the dark. Dark dissolution did not likely occur under our experimental conditions, even after hours of darkness, because TA at the algal surface was lower than in the bulk seawater, suggesting that dissolution was not the source of elevated CO_3^{2-} ions. The lower alkalinity at the surface in the dark could be due to nutrient uptake, as the uptake of phosphate and ammonium ions results in a decrease in alkalinity (Wolf-Gladrow et al., 2007). These results support the growing evidence that coralline algae have strong biotic control over their skeletal structure (Kamenos et al., 2013, 2016; Nash et al., 2015) and microenvironments where active calcification is occurring (Hofmann et al., 2016; Cornwall et al., 2017).

Arctic rhodoliths and crustose coralline algae control their surface chemistry actively. The surface pH dynamics upon illumination and darkening were rapid (within seconds), showing the presence of a light-driven proton pump. Further evidence for the presence of a proton pump was provided by the inhibition experiment with *L. glaciale*, which showed that despite inhibition of gross photosynthesis, there was no significant change in delta pH. Therefore, a process independent of photosynthesis
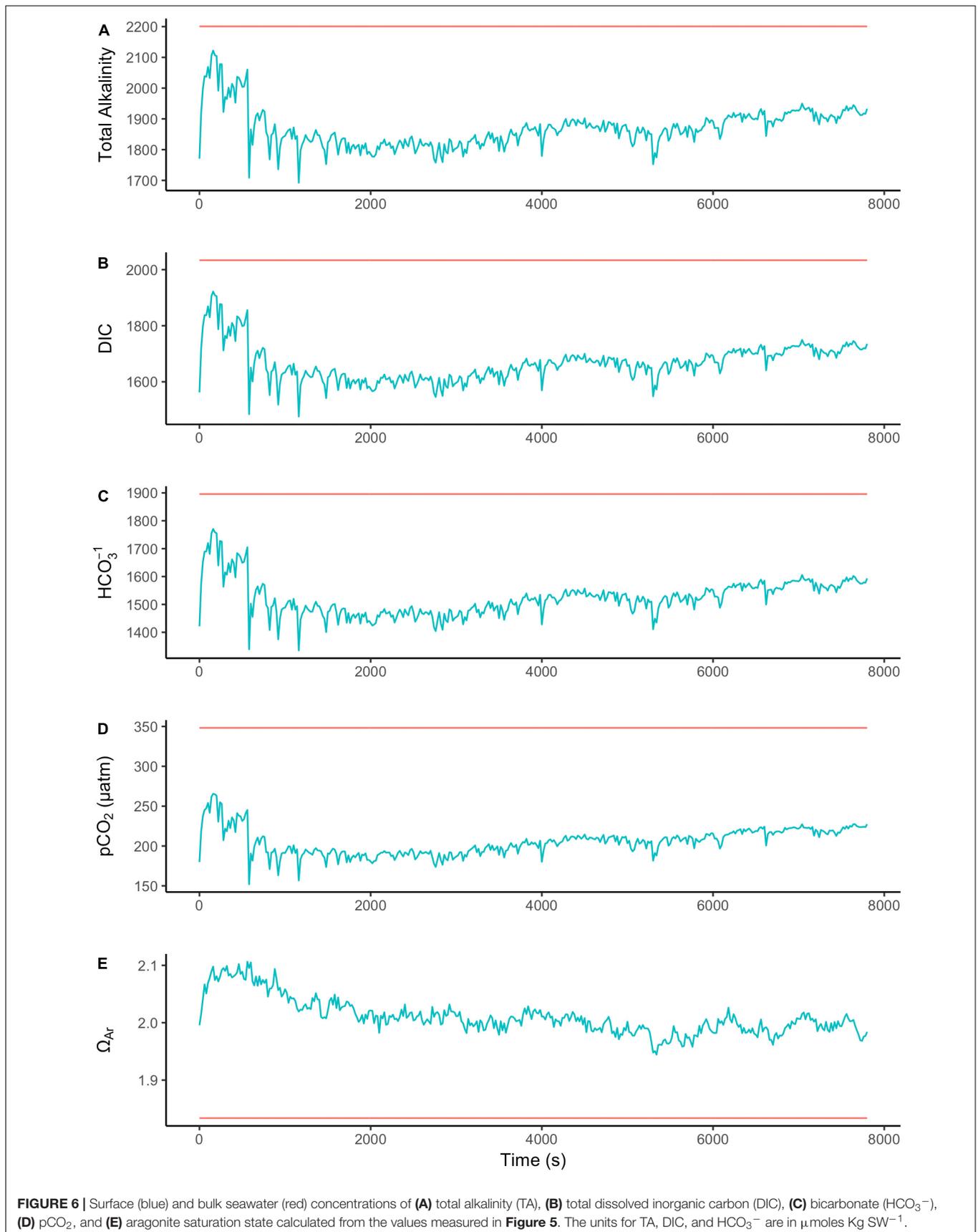
also influences the surface pH. Our observation differs from the recently proposed mechanism (Chrachri et al., 2018) in the marine diatom *Odontella sinensis*, whose surface pH was strongly inhibited by AZ, suggesting that surface pH is directly dependent on the rate of photosynthesis in this organism. Although photosynthesis in *L. glaciale* is strongly dependent on CA, it has an additional mechanism, a light-induced proton pump, that influences surface pH independently from photosynthesis. The same result has been reported for a tropical crustose coralline alga (Hofmann et al., 2016) and the calcifying green alga *Halimeda discoidea* (de Beer and Larkum, 2001). This photosynthesis independent, light-triggered proton pump may have been responsible for the rapid pH spikes we observed after turning off the light.

The surface carbonate ion dynamics were slower than the pH dynamics, suggesting that the carbonate dynamics were not only driven by pH. Because carbonate and bicarbonate are in almost instant equilibrium, the peaks in the carbonate dynamics likely represent rapid bicarbonate uptake by a carbon concentrating mechanism before a steady state is reached. The presence of a carbon concentrating mechanism in these algae has been recently supported by a separate study (Hofmann and Heesch, 2017). Additional support for the presence of a carbon concentrating mechanism utilizing HCO_3^-/H^+ co-transport was provided by our measurements during extended darkness. Despite the higher surface pH and CO_3^{2-} that we measured, the calculated TA

FIGURE 5 | Surface (blue) and bulk seawater (red) concentrations of **(A)** oxygen, **(B)** carbonate ion, and **(C)** pH measured during a period of extended darkness on a *P. tenue* individual from Spitsbergen. Note that time axis for oxygen is longer than for pH and carbonate.

at the algal surface during extended darkness was lower than the bulk seawater. This was explained by a strong reduction (ca. 75%) in the concentration of surface HCO_3^-, which was comparable to the reduction in protons (ca. 69%) associated with the elevated surface pH. Further evidence of HCO_3^- uptake

can be provided by modeling the seawater carbonate system. If we assume a photosynthetic quotient (O_2 released: CO_2 fixed) of 1 (but note that Chisholm (2000) reported a photosynthetic quotient of 1.05–1.48 for tropical coralline alga), we would expect the surface DIC concentration to decrease the same

FIGURE 6 | Surface (blue) and bulk seawater (red) concentrations of **(A)** total alkalinity (TA), **(B)** total dissolved inorganic carbon (DIC), **(C)** bicarbonate (HCO_3^-), **(D)** pCO_2, and **(E)** aragonite saturation state calculated from the values measured in **Figure 5**. The units for TA, DIC, and HCO_3^- are in μmoles Kg SW^{-1}.

magnitude as the surface O_2 concentration increased. On average, the O_2 concentration at the surface increased 10 µM under saturating light. Therefore, if we consider the bulk seawater has a pH of 8.15 and TA of 2200, the $[CO_3{}^{2-}]$ is 139 µM. An increase in pH to 8.2, which we observed, accompanied by a 10 µM decrease in DIC as CO_2 would result in a $[CO_3{}^{2-}]$ of 50 µM. On the other hand, a decrease in DIC as $HCO_3{}^-$ would result in a $[CO_3{}^{2-}]$ of 159 µM, which is comparable to the concentrations we observed at the surface of all the coralline algae investigated. Therefore, it is highly likely that the changes in surface chemistry are due to $HCO_3{}^-$ uptake coupled to H^+ co-transport or OH^- exchange. Our data, along with those from Comeau et al. (2013) and Hofmann et al. (2016) support the hypothesis by Borowitzka and Larkum (1987) that there is a $H^+/HCO_3{}^-$ symporter or $HCO_3{}^-/OH^-$ antiporter in coralline algae. Co-transport of $HCO_3{}^-$ and protons away from the calcifying surface and into the cell results in optimal conditions for calcification at the cell surface under both light and dark conditions, and elevated $HCO_3{}^-$ concentrations inside the cell neutralize the protons, providing an inorganic carbon source for photosynthesis in the light. This mechanism is in stark contrast to the mechanism proposed in some non-calcifying macroalgae, Characean algae, and freshwater flowering plants, where $HCO_3{}^-$ use is coupled to H^+ extrusion, producing acidic zones where the concentration of CO_2 is elevated due to the low pH and therefore diffuses into the cell (Moulin et al., 2011; Raven and Hurd, 2012). The H^+ extrusion must be accompanied by OH^- extrusion in alkaline zones. Our microsensor measurements do not support the presence of acidic or alkaline zones in coralline algae, although these zones are hypothesized to be much smaller than the diameter of a microsensor, and therefore cannot be accessed. Nevertheless, our results strongly suggest that $HCO_3{}^-$ is taken up directly, with either a net H^+ co-transport or net OH^- efflux, which results in a net increase in surface pH.

While this mechanism is easily explained under light conditions, it remains to be determined why and how Arctic coralline algae maintain elevated pH_S and $[CO_3{}^{2-}]_S$ in darkness. We hypothesize that these observations are a result of high rates of light independent carbon fixation, which is a common adaptation in polar macroalgae that facilitates their survival through the polar winter (Wiencke et al., 2009). Light independent carbon fixation (or β-carboxylation) is an anaplerotic pathway that involves the enzymes phosphoenol pyruvate carboxylase (PEPC) or phosphoenol pyruvate carboxykinase (PEPCK) to fix carbon dioxide (or bicarbonate) to the β-carbon of PEP or pyruvate. This process reduces carbon loss under darkness and produces important metabolites, such as amino acids. High rates of light independent carbon fixation would explain the continued inorganic carbon uptake (in this case as $HCO_3{}^-$) and elevated surface pH in the dark, despite oxygen consumption resulting from dark respiration. Further evidence for this hypothesis can be seen in the data from Hofmann and Heesch (2017), who reported the total and organic $^{13}C{:}^{12}C$ fractionation in Atlantic rhodoliths. The organic fraction $\partial^{13}C$ signatures of Arctic rhodoliths, including specimens from the same collection sites used in this study, deviated from the linear trend with latitude. The Arctic rhodoliths had organic

material more enriched in ^{13}C than would be expected based on the latitudinal trend, which may be due to higher rates of anaplerotic reactions that result in ^{13}C enriched carboxyl carbons (Savidge and Blair, 2004). Although the CO_2 concentration at the algal surface (based on the measured pH and $CO_3{}^{2-}$ concentrations) was lower than the bulk seawater and hence suggests CO_2 uptake by the alga in the dark, our hypothesis is at this time speculative, as we did not directly measure CO_2 uptake in the dark. Additional possibilities for dark CO_2 uptake [e.g., carbamoyl phosphate synthase (Raven et al., 1990)] cannot be excluded. Further studies measuring direct CO_2 fluxes would be necessary to confirm our hypothesis.

CONCLUSION

In conclusion, our results suggest that Arctic corallines have strong biological control over their surface chemistry, where active calcification occurs. High rates of light independent carbon fixation are likely an adaptive strategy in Arctic coralline algae for limiting carbon loss during long periods of darkness, and additionally create a microenvironment that prevents dissolution in the dark. Our results suggest that net dissolution in the dark is not currently a threat to Arctic coralline algae during the summer. However, long exposure to darkness resulted in a surface pH below seawater pH, suggesting that dissolution could still occur during winter. These unique physiological mechanisms likely play an important role in facilitating the survival of Arctic coralline algae under harsh conditions, but further studies will be needed to determine if these mechanisms could facilitate adaptation to ocean acidification in the future, which would have important implications for Arctic marine ecosystems.

DATA AVAILABILITY

The datasets generated during and/or analyzed during the current study are available from the corresponding author upon reasonable request.

AUTHOR CONTRIBUTIONS

LH designed and carried out the experiment and wrote the manuscript. KS collected the samples from Greenland and edited the manuscript. DdB edited the manuscript.

FUNDING

SUPPLEMENTARY MATERIAL

The Supplementary Material for this article can be found online at: https://www.frontiersin.org/articles/10.3389/fpls.2018.01416/full#supplementary-material

FIGURE S1 | Light/dark dynamics of $[CO_3^{2-}]$ in *P. tenue*.

FIGURE S2 | Light/dark dynamics and extended darkness $[CO_3^{2-}]$ in *L. tophiforme*.

FIGURE S3 | Surface pH and $[O_2]$ of *P. tenue* during extended darkness.

FIGURE S4 | Surface $[CO_3^{2-}]$ and pH of *L. tophiforme* during extended darkness.

FIGURE S5 | Surface $[O_2]$ and pH before and after AZ addition.

FIGURE S6 | Delta pH at the surface of *L. glaciale* before and after AZ addition.

FIGURE S7 | Effect of AZ on gross photosynthesis in *L. glaciale*.

TABLE S1 | Thickness of the diffusional boundary layer at different locations on the thalli.

TABLE S2 | T-tests comparing surface and bulk $[O_2]$ for each species.

REFERENCES

Al-Horani, F. A., Al-Moghrabi, S. M., and De Beer, D. (2003). The mechanism of calcification and its relation to photosynthesis and respiration in the scleractinian coral *Galaxea fascicularis*. *Mar. Biol.* 142, 419–426. doi: 10.1007/s00227-002-0981-8

Amado-Filho, G. M., Moura, R. L., Bastos, A. C., Salgado, L. T., Sumida, P. Y., Guth, A. Z., et al. (2012). Rhodolith beds are major CaCO 3 BIO-factories in the tropical south West Atlantic. *PLoS One* 7:e35171. doi: 10.1371/journal.pone.0035171

Borowitzka, M. A., and Larkum, A. W. D. (1976). Calcification in the green alga Halimeda: III. The sources of inorganic carbon for photosynthesis and calcification and a model of the mechanism of calcification. *J. Exp. Bot.* 27, 879–893. doi: 10.1093/jxb/27.5.879

Borowitzka, M. A., and Larkum, A. W. D. (1977). Calcification in the green alga Halimeda. I. An ultrastructure study of thallus developement. *J. Phycol.* 13, 6–16. doi: 10.1111/j.1529-8817.1977.tb02879.x

Borowitzka, M. A., and Larkum, A. W. D. (1987). Calcification in algae: mechanisms and the role of metabolism. *CRC. Crit. Rev. Plant Sci.* 6, 1–45. doi: 10.1080/07352688709382246

Büdenbender, J., Riebesell, U., and Form, A. (2011). Calcification of the Arctic coralline red algae *Lithothamnion glaciale* in response to elevated CO 2. *Mar. Ecol. Prog. Ser.* 441, 79–87. doi: 10.3354/meps09405

Chisholm, J. R. M. (2000). Calcification by crustose coralline algae on the northern great barrier reef, Australia. *Limnol. Oceanogr.* 45, 1476–1484. doi: 10.4319/lo.2000.45.7.1476

Chrachri, A., Hopkinson, B. M., Flynn, K., Brownlee, C., and Wheeler, G. L. (2018). Dynamic changes in carbonate chemistry in the microenvironment around single marine phytoplankton cells. *Nat. Commun.* 9:74. doi: 10.1038/s41467-017-02426-y

Comeau, S., Carpenter, R. C., and Edmunds, P. J. (2013). Coral reef calcifiers buffer their response to ocean acidification using both bicarbonate and carbonate. *Proc. R. Soc. B* 280:20122374. doi: 10.1098/rspb.2012.2374

Cornwall, C. E., Comeau, S., and McCulloch, M. T. (2017). Coralline algae elevate pH at the site of calcification under ocean acidification. *Glob. Chang. Biol* 23, 4245–4256. doi: 10.1111/gcb.13673

Cornwall, C. E., Hepburn, C. D., Pilditch, C. A., and Hurd, C. L. (2013). Concentration boundary layers around complex assemblages of macroalgae: implications for the effects of ocean acidification on understory coralline algae. *Limnol. Oceanogr.* 58, 121–130. doi: 10.4319/lo.2013.58.1.0121

Cornwall, C. E., Pilditch, C. A., Hepburn, C. D., and Hurd, C. L. (2015). Canopy macroalgae influence understorey corallines' metabolic control of near-surface pH and oxygen concentration. *Mar. Ecol. Prog. Ser.* 525, 81–95. doi: 10.3354/meps11190

Cui, S., He, J., He, P., Zhang, F., Lin, L., and Ma, Y. (2013). The adaptation of Arctic phytoplankton to low light and salinity in Kongsfjorden (Spitsbergen). *Adv. Polar Sci.* 23, 19–24. doi: 10.3724/SP.J.1085.2012.00019

de Beer, D., Bissett, A., de Wit, R., Jonkers, H., Köhler-Rink, S., Nam, H., et al. (2008). A microsensor for carbonate ions suitable for microprofiling in freshwater and saline environments. *Limnol. Oceanogr. Methods* 6, 532–541. doi: 10.4319/lom.2008.6.532

de Beer, D., and Larkum, A. W. D. (2001). Photosynthesis and calcification in the calcifying algae *Halimeda discoidea* studied with microsensors. *Plant Cell Environ.* 24, 1209–1217. doi: 10.1046/j.1365-3040.2001.00772.x

Donald, H. K., Ries, J. B., Stewart, J. A., Fowell, S. E., and Foster, G. L. (2017). Boron isotope sensitivity to seawater pH change in a species of *Neogoniolithon coralline* red alga. *Geochim. Cosmochim. Acta* 217, 240–253. doi: 10.1016/j.gca.2017.08.021

Eilers, P., and Peeters, J. (1988). A model for the relationship between light intensity and the rate of photosynthesis in phytoplankton. *Ecol. Modell.* 42, 199–215. doi: 10.1016/0304-3800(88)90057-9

Foster, M. S. (2001). Rhodoliths: between rocks and soft places. *J. Phycol.* 37, 659–667. doi: 10.1046/j.1529-8817.2001.00195.x

Gattuso, J. P., Allemand, D., and Frankignoulle, M. (1999). Photosynthesis and calcification at cellular, organismal and community levels in coral reefs: a review on interactions and control by carbonate chemistry. *Am. Zool.* 39, 160–183. doi: 10.1093/icb/39.1.160

Hajime, I., and Kudoh, S. (1997). Characteristics of water in Kongsfjorden, Svalbard. *Proc. NIPR Symp. polar Meteorol. Glaciol.* 11, 211–232. doi: 10.1016/j.scitotenv.2011.03.015

Han, C., Cai, W.-J., Wang, Y., and Ye, Y. (2014). Calibration and evaluation of a carbonate microsensor for studies of the marine inorganic carbon system. *J. Oceanogr.* 70, 425–433. doi: 10.1007/s10872-014-0243-7

Hanelt, D., Tüg, H., Bischof, K., Groß, C., Lippert, H., Sawall, T., et al. (2001). Light regime in an Arctic fjord: a study related to stratospheric ozone depletion as a basis for determination of UV effects on algal growth. *Mar. Biol.* 138, 649–658. doi: 10.1007/s002270000481

Hofmann, L. C., and Bischof, K. (2014). Ocean acidification effects on calcifying macroalgae. *Aquat. Biol.* 22, 261–279. doi: 10.3354/ab00581

Hofmann, L. C., and Heesch, S. (2017). Latitudinal trends in stable isotope signatures and carbon concentrating mechanisms of northeast Atlantic rhodoliths. *Biogeosci. Discuss.* doi: 10.5194/bg-2017-399

Hofmann, L. C., Koch, M., and De Beer, D. (2016). Biotic control of surface pH and evidence of light-induced H^+ pumping and Ca^{2+}-H^+ exchange in a tropical crustose coralline alga. *PLoS One* 11:e0159057. doi: 10.1371/journal.pone.0159057

Hurd, C. L., Cornwall, C. E., Currie, K., Hepburn, C. D., McGraw, C. M., Hunter, K. A., et al. (2011). Metabolically induced pH fluctuations by some coastal calcifiers exceed projected 22nd century ocean acidification: a mechanism for differential susceptibility? *Glob. Chang. Biol.* 17, 3254–3262. doi: 10.1111/j.1365-2486.2011.02473.x

Jørgensbye, H. I. Ø., and Halfar, J. (2017). Overview of coralline red algal crusts and rhodolith beds (Corallinales, Rhodophyta) and their possible ecological

importance in Greenland. *Polar Biol* 40, 517–531. doi: 10.1007/s00300-016-1975-1

Kamenos, N. A., Burdett, H. L., Aloisio, E., Findlay, H. S., Martin, S., Longbone, C., et al. (2013). Coralline algal structure is more sensitive to rate, rather than the magnitude, of ocean acidification. *Glob. Chang. Biol.* 19, 3621–3628. doi: 10.1111/gcb.12351

Kamenos, N. A., Perna, G., Gambi, M. C., Micheli, F., and Kroeker, K. J. (2016). Coralline algae in a naturally acidified ecosystem persist by maintaining control of skeletal mineralogy and size. *Proc. R. Soc. London B Biol. Sci.* 283:20161159. doi: 10.1098/rspb.2016.1159

Laudien, J., Sahade, R. J., and Schwanitz, M. (2014). *Water Temperature at Time Series Station Kongsfjordneset-2, Spitsbergen, Kongsfjorden, Arctic in 2012/2013.* Bremerhaven: Alfred Wegener Institute, Helmholtz Center for Polar and Marine Research, doi: 10.1594/PANGAEA.830142

McConnaughey, T. (1991). Calcification in Chara corallina: CO_2 hydroxylation generates protons for bicarbonate assimilation. *Limnol. Oceanogr.* 36, 619–628. doi: 10.4319/lo.1991.36.4.0619

McConnaughey, T. A. (1989). "Biomineralization Mechanisms," in *Origin, Evolution, and Modern Aspects of Biomineralization in Plants and Animals*, ed. R. E. Crick (Boston, MA: Springer), 57–73. doi: 10.1007/978-1-4757-6114-6

McCoy, S. J., and Kamenos, N. A. (2015). Coralline algae (Rhodophyta) in a changing world: integrating ecological, physiological, and geochemical responses to global change. *J. Phycol.* 51, 6–24. doi: 10.1111/jpy.12262

McCoy, S. J., and Ragazzola, F. (2014). Skeletal trade-offs in coralline algae in response to ocean acidification. *Nat. Clim. Chang.* 4, 719–723. doi: 10.1038/nclimate2273

Moulin, P., Andría, J. R., Axelsson, L., and Mercado, J. M. (2011). Different mechanisms of inorganic carbon acquisition in red macroalgae (Rhodophyta) revealed by the use of TRIS buffer. *Aquat. Bot.* 95, 31–38. doi: 10.1016/j.aquabot.2011.03.007

Nash, M. C., Opdyke, B. N., Troitzsch, U., Russell, B. D., Adey, W. H., Kato, A., et al. (2013). Dolomite-rich coralline algae in reefs resist dissolution in acidified conditions. *Nat. Clim. Chang.* 3, 268–272. doi: 10.1038/nclimate1760

Nash, M. C., Uthicke, S., Negri, A. P., and Cantin, N. E. (2015). Ocean acidification does not affect magnesium composition or dolomite formation in living crustose coralline algae, *Porolithon onkodes* in an experimental system. *Biogeosci. Discuss* 12, 1373–1404. doi: 10.5194/bgd-12-1373-2015

Nelson, W. A. (2009). Calcified macroalgae critical to coastal ecosystems and vulnerable to change: a review. *Mar. Freshw. Res.* 60, 787–801. doi: 10.1071/MF08335

Noguchi, K., Gel, Y. R., Brunner, E., and Konietschke, F. (2012). nparLD: an R software package for the nonparametric analysis of longitudinal data in factorial experiments. *J. Stat. Softw* 50, 1–23. doi: 10.18637/jss.v050.i12

Ragazzola, F., Foster, L. C., Form, A. U., Büscher, J., Hansteen, T. H., and Fietzke, J. (2013). Phenotypic plasticity of coralline algae in a high CO world. *Ecol. Evol.* 3, 3436–3446. doi: 10.1002/ece3.723

Ragazzola, F., Foster, L. C., Jones, C. J., Scott, T. B., Fietzke, J., Kilburn, M. R., et al. (2016). Impact of high CO_2 on the geochemistry of the

coralline algae *Lithothamnion glaciale*. *Sci. Rep.* 6:20572. doi: 10.1038/srep20572

Raven, J. A., and Hurd, C. L. (2012). Ecophysiology of photosynthesis in macroalgae. *Photosynth. Res.* 113, 105–125. doi: 10.1007/s11120-012-9768-z

Raven, J. A., Johnston, A. M., and Macfarlane, J. J. (1990). "Carbon Metabolism," in *Biology of the Red Algae*, eds K. M. Cole and R. G. Sheath (Cambridge: Cambridge University Press), 171–202.

Revsbech, N. P. (1989). An oxygen microsensor with a guard cathode. *Limnol. Oceanogr.* 34, 474–478. doi: 10.4319/lo.1989.34.2.0474

Revsbech, N. P., and Jørgensen, B. B. (1983). Photosynthesis of benthic microflora measured with high spatial resolution by the oxygen microprofile method: Capabilities and limitations of the method. *Limnol. Oceanogr.* 28, 749–756. doi: 10.4319/lo.1983.28.4.0749

Revsbech, N. P., and Jørgensen, B. B. (1986). "Microelectrodes: their use in microbial ecology," in *Advances in Microbial Ecology*, ed. K. Marshall (New York, NY: Springer), 293–352.

Savidge, W. B., and Blair, N. E. (2004). Patterns of intramolecular carbon isotopic heterogeneity within amino acids of autotrophs and heterotrophs. *Oecologia* 139, 178–189. doi: 10.1007/s00442-004-1500-z

Shadwick, E. H., Trull, T. W., Thomas, H., Gibson, J. A. E., Stouffer, R. J., Manabe, S., et al. (2013). Vulnerability of polar oceans to anthropogenic acidification: comparison of arctic and antarctic seasonal cycles. *Sci. Rep.* 3, 660–662. doi: 10.1038/srep02339

Steinacher, M., Joos, F., Frölicher, T. L., Plattner, G.-K., and Doney, S. C. (2009). Imminent ocean acidification in the Arctic projected with the NCAR global coupled carbon cycle-climate model. *Biogeosciences* 6, 515–533. doi: 10.5194/bg-6-515-2009

Van Der Heijden, L., and Kamenos, N. A. (2015). Reviews and syntheses: calculating the global contribution of coralline algae to total carbon burial. *Biogeosciences* 12, 6429–6441. doi: 10.5194/bg-12-6429-2015

Wiencke, C., Gó Mez, I. N., and Dunton, K. (2009). Phenology and seasonal physiological performance of polar seaweeds. *Bot. Mar.* 52, 585–592. doi: 10.1515/BOT.2009.078

Wolf-Gladrow, D. A., Zeebe, R. E., Klaas, C., Körtzinger, A., and Dickson, A. G. (2007). Total alkalinity: the explicit conservative expression and its application to biogeochemical processes. *Mar. Chem.* 106, 287–300. doi: 10.1016/J.MARCHEM.2007.01.006